The Journal of Experimental Biology 212, 3478-3489
Published by The Company of Biologists 2009
doi:10.1242/jeb.033217

Waveform diversity of electric organ discharges: the role of electric organ auto-excitability in *Gymnotus* spp.

Alejo Rodríguez-Cattáneo and Angel Ariel Caputi*

Departamento de Neurociencias Integrativas y Computacionales, Instituto de Investigaciones Biológicas Clemente Estable, Montevideo, Uruguay, Av. Italia 3318, Montevideo, Uruguay

*Author for correspondence (angel@iibce.edu.uy)

Accepted 28 July 2009

SUMMARY

This article shows that differences in the waveforms of the electric organ discharges (EODs) from two taxa are due to the different responsiveness of their electric organs (EOs) to their previous activity (auto-excitability). We compared *Gymnotus omarorum* endemic to Uruguay (35° South, near a big estuary), which has four components in the head to tail electric field (V_1 to V_4), with *Gymnotus* sp. endemic to the south of Brazil, Paraguay and Argentinean Mesopotamia (25° South, inland), which shows a fifth component in addition to the others (V_5). We found that: (a) the innervation pattern of the electrocytes, (b) the three earlier, neurally driven, EOD components (V_1 to V_3), and (c) their remnants after curarisation were almost identical in the two taxa. The equivalent electromotive forces of late components (V_4 and V_5) increased consistently as a function of the external current associated with the preceding component and were abolished by partial curarisation in both taxa. Taken together these data suggest that these components are originated in the responses of the electrocytes to longitudinal currents through the EO. By using a differential load procedure we showed that V_4 in *G. omarorum* responded to experimental changes in its excitation current with larger amplitude variations than V_4 in *Gymnotus* sp. We conclude that the differences in the EOD phenotype of the two studied taxa are due to the different EO auto-excitability. This, in turn, is caused either by the different expression of a genetic repertoire of conductance in the electrocyte membrane or in the wall of the tubes forming the EO.

Key words: electric organ, evolution, electrocyte, intrinsic properties, electric fish.

INTRODUCTION

The discovery of weak continuous electric organ discharges [EODs (Lissmann, 1951)] emitted by *Gymnarchus niloticus* was the first step for solving the question posed by Charles Darwin (Darwin, 1866) concerning the function and evolution of electric organs (EOs). Lissmann's article was followed by a series of subsequent articles showing that: (a) the EOD emitted by a fish triggers behavioural responses in other fish (Mohres, 1957); (b) fish can detect and discriminate electromagnetic signals (Lissmann, 1958; Lissmann and Machin, 1958; Machin and Lissmann, 1960); and (c) there are sensory receptor organs tuned for the species-specific EOD waveform (Bullock et al., 1961). These studies beautifully demonstrated that the EOs and their control system constitute a paradigmatic specialisation of the motor system, whose function is to provide a carrier for sensory signals (Bennett and Grundfest, 1959). The theoretical framework already elaborated in the pioneer papers (Lissmann, 1958; Lissmann and Machin, 1958; Machin and Lissmann, 1960) set the basis for understanding this sensory modality and its two roles in animal life: active electrosensory exploration of the environment and electrocommunication with conspecifics.

One of the most salient characteristics of the electric fields generated by electric fish is the species specificity of its waveforms (Coates et al., 1954; Bennett and Grundfest, 1959). Beyond constituting a taxonomic sign for species identification, the biological role of species specificity of the EOD is still a matter of discussion. Several non-exclusive hypotheses have been raised about this point. Some authors suggest that main driving force in the evolution of EOD waveform is a process of cryptic adaptation in order to avoid predation (Stoddard, 1999; Stoddard, 2002). This process tends to increase the number of waves produced in a given time and the EOD power spectra are shifted to a higher frequency range. Other authors suggest that species-specific waveform has a crucial role for species recognition in mating and reproduction (Crampton and Albert, 2005; Albert and Crampton, 2005). Ecologically co-occurring species of gymnotiforms (e.g. *Gymnotus carapo* and *Gymnotus coropinae*) often exhibit non-overlapping ranges of far field power spectra suggesting that these species may be able to recognise and discriminate each other on the basis of frequency components of the electrocommunication carrier. However, the ranges of the power spectra of various species co-occurring at floodplain habitats of Central Amazon overlap. A wavelet 'signal space' representing features of the head to tail EOD waveform suggests that these species may recognise and discriminate each other on the basis of both frequency and temporal components of the electrocommunication carrier (Crampton et al., 2008). Finally, seasonal control of EOD waveform by environmental and hormonal factors may result in carrier modulation and thus result in gender and dominance signs and/or signals (Bass and Hopkins, 1983; Hopkins et al., 1990; Silva et al., 2002).

Species specificity of the EOD is provided by the evolution of different electromotor control mechanisms and effectors responsible for this control (Bennett and Grundfest, 1959; Bennett, 1971; Bass, 1986; Caputi, 1999; Caputi et al., 2005). While the EOD waveform of African electric fish (Mormyridae) is characteristic of the responses of a homogeneous population of synchronously activated electrogenic units (Hopkins, 1999), American electric fish (Gymnotiforms) show a combination of

strategies yielding more complex EOD waveforms. Gymnotiforms exhibit a relatively long EO, located in the ventral part of the body from the anal pore to the tip of the tail, covering about 90% of the fish's body length. These EOs can be myogenic or neurogenic, depending on the species. Myogenic organs are composed of longitudinal tubes of connective tissue in which the electrogenic units are aligned in an orderly manner, much like the batteries in a hand flash light (torch) (Bennett and Grundfest, 1959; Couceiro and De Almeida, 1961; Trujillo-Cenóz et al., 1984; Trujillo-Cenóz and Echague, 1989). Each of these electrogenic units (known as electrocytes) is a muscle-derived syncitium, which has lost its contractile machinery but has developed the ability to generate species-specific electrical responses (Bennett, 1971; Zakon et al., 2008). In the species with myogenic organs, the EOD can take the form of a sequence of brief pulses separated by silent intervals 4–100 times longer than the duration of the pulse (pulse-emitting fish) or by intervals similar in duration to the pulse (wave-emitting fish). Neurogenic organs, however, are composed of the axons of spinal electromotoneurons, which run longitudinally and are packed in an orderly manner along extended portions of the fish body (Bennett, 1971). All known species having neurogenic organs are wave-emitting fish.

In most gymnotid pulse species, the intrinsic properties, the innervation and the activation time of the electrocytes are dependent on electrocyte location (Caputi et al., 1989; Caputi et al., 1994). Thus, the EODs of pulse-emitting species can be likened to complex motor acts characterised by fixed spatio-temporal patterns of electromotive forces. Their comparative analysis may be a useful window for identifying traits in their evolution. We have postulated that waveform diversity arises from either: (a) variations in the intrinsic properties or innervation patterns of the electrocytes; (b) variations in the activation timing of different regions of the EO and the rostral and caudal faces of the individual electrocytes; or (c) the additional occurrence of neurogenic electrogenesis. We also suggested that the 'labile links' in the determination of waveform evolution will be related to diversity of this sort in the mechanisms underlying electrogenesis (Rodríguez-Cattáneo et al., 2008).

The most widely accepted hypothesis on waveform generation for pulse gymnotids states that two types of components can be distinguished according to their generation mechanism (Bennett, 1971; Caputi et al., 2005).

The first type, direct neurally driven components (V_1, V_2 and V_3 in *G. omarorum*) originate as the sum of electrocyte responses to a synchronised neural volley that synaptically activates a set of similarly oriented membrane patches. This causes first a synaptic depolarisation of the innervated faces and, potentially, the subsequent firing of a spike in the post-synaptic electrocyte. For example, in *G. omarorum*, V_1 originates from the sum of post-synaptic potentials generated at the rostral faces of the abdominal electrocytes; V_2 originates from the sum of action potentials generated at the rostral faces of the electrocytes in the mid-body (central) region; and V_3 originates from the sum of action potentials generated at the caudal faces of the electrocytes all along the fish's body (Macadar et al., 1989; Caputi et al., 1989).

The second type of component contributing to the EOD waveform, referred to here as indirectly driven components, is a consequence of the electrocyte membrane activation by longitudinal currents flowing along the EO. The action currents associated with the spikes generating V_3 flow along the EO stimulating the opposite membranes of the electrocyte and passing through the EO as a whole triggering a second spike, which in turn gives rise to V_4 (Bennett and Grundfest, 1959; Macadar et al., 1989; Caputi et al., 1989). A similar process gives rise to V_5 in other fish. The electrocytes of *G. omarorum* have a complex repertoire of channels that are differently distributed in the rostral and caudal faces of the electrocytes (Sierra et al., 2005; Sierra et al., 2007) and this repertoire thus shapes the contribution of each individual electrocyte to the EOD. The longitudinal flow of current is not a local process restricted to a single electrocyte but rather it is a process dependent on the ability of the EO to funnel (and therefore to summate) the currents generated by the neighbouring electrocytes (Albe-Fessard and Buser, 1950). This mechanism, besides depending on excitability, depends also on inter-electrocyte distance and on the space constant of each tube, which in turn depends on the resistances of the connective sheath and the jelly tissue in between the electrocytes.

Thus, the ability of the EO as a whole to generate new components as described above can be altered by the presence of an external load. The electromotive force (EMF) of the equivalent source for the indirectly driven components is highly dependent on the load resistance and consequently is not linear. This is the case of the mormyrid *Gnathonemus petersii* (Bell et al., 1976) and the gymnotid *Brachyhypopomus pinnicaudatus* (Caputi et al., 1998).

In this article we describe an example of waveform divergence in two parapatric taxonomic units of *Gymnotus* spp. endemic to neighbouring regions of Latin America: *Gymnotus omarorum* (from the south of Uruguay) and *Gymnotus* sp. (from the west of Rio Grande do Sul, Paraguay and north-eastern Argentina). We found that the waveform differences are mainly determined by the responsiveness of the EO to its previous activity (auto-excitability).

MATERIALS AND METHODS

Forty specimens of *Gymnotus omarorum* (Richer de Forges et al., 2009) and twenty specimens of a still undescribed species *Gymnotus* sp. were utilised in this study. Both kinds of fish are called 'morena' in the local fisherman's jargon. *Gymnotus* sp. were bought from local dealers in La Paz, Argentina (in March 2008 and 2009) and were presumably recently caught in the affluent of the Paraná River near the border between Paraguay and Argentina. *Gymnotus omarorum* was captured by the authors in the Laguna del Cisne, Uruguay, in all four seasons of the year from March 2008 to April 2009. In this study, all potentially harmful procedures were conducted under anaesthesia, following IIBCE's regulations for the use of experimental animals and the guidelines of the Comisión Honoraria de Experimentación Animal of the Universidad de la República (CHEA), and the Society for Neuroscience.

Anatomy and innervation of the electrogenic tissue

The structure of the EO and the distribution of the thin nerve bundles, as well as the arrangement of the electromotor nerve terminals on the surface of the electrocytes, were studied using silver impregnated samples.

Fish were decapitated under deep terminal anaesthesia (MS222 250 mg l^{-1}, until gilling movements and the EOD ceased). After a combined fixation and decalcification step by immersion in De Castro's solution [formulae in Ramón y Cajal and De Castro (Ramón y Cajal and De Castro, 1933)], portions of the fish were silver impregnated by immersion in $AgNO_3$, 1.5%, for 7 days at 37°C, and this was subsequently reduced in formaldehyde-hydroquinone. We studied: (a) the abdominal walls; (b) a portion of the mid-body region about 50% along the length of the fish body; and (c) a portion of the tail (caudal 10%). Tissues were embedded in a soft mixture of epoxy resin and sectioned using a sliding microtome (30 μm thick) either frontally or parasagitally. Sections were explored under the

light microscope, and digital images were made using different optical and CCD resolutions.

Measurements of the EOD-associated electric fields

Head to tail electric fields produced by the EOD were recorded with the fish resting in the middle of a net pen running between the centres of the short walls (28 cm) of a plastic tank (48×28 cm, filled with water up to 4 cm depth, conductivity 30 μs cm^{-1}, temperature 24°C). The back and forth movements of the fish were minimised using stitches to adjust the net to the shape of the body. The longitudinal head to tail EOD (htEOD) fields, recorded using two stainless steel electrodes, placed on the middle of each of the short walls of the tank, one facing the head and the other facing the tail. Voltage between the electrodes was measured using a high-input impedance, high-gain, differential amplifier (10–20 kHz band-pass filter, floating ground). Recorded waveforms were sampled (25–50 kHz, depending on the number of channels recorded, 16 bits) and displayed on a computer screen.

Measurements of the equivalent source parameters

To evaluate the spatio-temporal pattern of equivalent EMF for the fish body, we used the air-gap technique (Coates et al., 1937; Cox and Coates, 1938; Bell et al., 1976; Caputi et al., 1993), which consists of the simultaneous recording of the voltage drop generated by different portions of the fish's body when isolated in air. In the simplest version, this procedure gives a holistic estimate of the EMF and internal resistance of the fish's body (R_i) by recording the drop in voltage (V) across a variable loading resistor connected to the head and the tail in such a way that all of the external current (I) generated by the fish body is funnelled through the load. The EMF is then calculated as the ordinate intersection of the function relating V and I:

$$V = EMF - R_i \times I,$$

where R_i is the equivalent internal resistance in series with the EMF. It corresponds to the resultant from a parallel array of the resistances of electrogenic and non-electrogenic tissues (Caputi et al., 1989).

Like the htEOD recorded in water, the htEOD recorded in air is a holistic estimate that lacks the necessary spatio-temporal dimensions to describe the electrogenic source in gymnotids. This is because different portions of the fish body emit regional EODs with different waveforms. In these fish the EOs are extended, non-homogeneous structures in which different regions generate different waveforms and, in the case of the wave components generated by non-innervated faces of electrocytes, the voltage *vs* current plot frequently yields a non-linear relationship, and the EMF is load dependent (Bell et al., 1976; Caputi et al., 1998). Therefore, we used complementary methods to explore spatial waveform pattern of the EOD and the auto-excitability of the EO.

Exploration of the spatial waveform pattern

For multiple air gap exploration (Caputi et al., 1993), fish were suspended in air using a custom made electrode array consisting of seven parallel wires perpendicular to the main axis of the body, placed in contact with the skin, one at each extreme of the fish and the others at the limits of the explored regions. Seven regions of the fish body were considered: the head, the abdomen and five consecutive caudal portions (each one equivalent to one-seventh of the fish's length). Voltages recorded between consecutive pairs of wires were amplified to reach adequate amplitude for similar quantization (always larger than 8 bits) and sampled at 25 kHz. In the air gap condition, there was no load, so voltage recordings were considered to be good estimators of the equivalent EMFs generated by different portions of the fish's body. However, this was not the case for all wave components because the equivalent sources of some indirectly neurally driven components are not linear.

The spatio-temporal pattern under partial curarisation

The objective of curarisation was to show the similarity of the EOD remnant when the electromotor drive diminishes under the synaptic threshold for eliciting the contribution of electrocyte action potentials to the EOD. This is a necessary condition to verify that the mechanisms involved in the generation of V_1, V_2 and V_3 are similar in both species and that the main differences are in the mechanism underlying V_4. Curarisation allowed us to compare the remnants of the EOD wave components when they achieve a stabilised waveform in which V_4 and V_5 are absent. We used a slow-acting, long-lasting, nicotinic antagonist (d-tubocurarine) to block the electrocyte's end plates in a competitive and progressive way. As it is known from previous studies (Caputi et al., 1989; Caputi et al., 1994; Caputi et al., 1998; Caputi and Aguilera, 1996), the effect of d-tubocurarine occurs in two phases. During the first phase, the EOD become initially disorganised, showing a decay in amplitude and an increase in duration of the components. At the acme of disorganisation phase bursts of supernumerary wavelets following the main EOD are frequently observed. If curare concentration is enough this disorganisation phase is followed by a stable phase where the EOD remnant becomes a new stereotyped waveform that decays in amplitude until all post-synaptic activity is blocked. At this stabilised partial curarisation stage, each of these remnants reflect the sub-threshold post-synaptic activity in which timing, shape, amplitude and spatial origin along the fish body are characteristics of the species.

In three individuals of each taxon we compared the regional EOD in the intact fish with that resulting from partial curarisation at the stable phase (0.5 μg g^{-1} of d-tubocurarine, i.m.). Fish tolerated this dose without stopping breathing or modifying their EOD rate but showed large changes in their EODs. We compared recordings, obtained from three portions of the fish (1 or 2 cm long depending on the experiment) located in the abdominal region (between the anal papilla and the origin of the anal fin), at the central region (about the centre of the fish length) and at the tail region (at the most caudal possible portion).

Exploration of EO auto-excitability

We employed the method described by Bell et al. (Bell et al., 1976) to explore the efficacy of the longitudinal currents generating V_3 for eliciting V_4 at the tail region. This method consists of splitting the load into two parallel 'one way' paths of opposite direction using Germanium diodes. While one diode allows the current generating V_3 (I_3) to flow through an externally controlled resistive path and blocks the current generating V_4 (I_4), the other diode allows the circulation of I_4 through another externally controlled path, blocking I_3. It is important to note that when the absolute values of peak voltages are lower than the cut-off threshold of the diodes (300 mV) current does not circulate in any direction. However, when the absolute values of peak voltages are larger than the diode threshold, they are controlled by the external load. We used an 11-position step switch to modify an external load connected in series with a diode oriented in such a way that allowed only the flow of I_3 (R2, Fig. 8A). Thus, for a given position of the step switch we clamped the peak value of I_3. For each of the 11 positions of the switch (i.e. for each value of I_3) we explored the voltage–current relationship of V_4 by varying the resistance of a rheostat connected in series

with the second diode (R1, Fig. 8A). At the end of this series of experiments, we obtained 11 characteristic curves, one for each position of the switch. Because we found that voltage current was well fitted by a linear decreasing function (see Results) we were able to estimate the EMF generating V_4 (EMF_4) for each clamped value of I_3. In order to compare results from fish of different sizes, we constructed an index of EO auto-excitability defined as the ordinate value of the relative EMF_4. This is equivalent to the quotient between minimum EMF_4 (for very large load resistances, near open circuit) and the maximum EMF_4 (for very low load resistance, near short circuit).

RESULTS

The htEOD in water

The specimens of *G. omarorum* and *Gymnotus* sp. were very similar in their external morphology. Their EOD waveform recorded head to tail in water (24–26°C, 20–50 μS cm^{-1}), although similar, showed the following differences: (a) while the EOD waveform of *G. omarorum* exhibited four components [V_1 to V_4 in Fig. 1A (Trujillo-Cenóz et al., 1984)], that of *Gymnotus* sp. exhibited five, adding a late smooth positive component (V_1 to V_5 in Fig. 1B); (b) the relative peak of V_4 is larger in *Gymnotus* sp. (V_4/V_3 ratios were 0.463+0.033 and 0.854+0.039, mean and standard deviation for *G. omarorum* and *Gymnotus* sp., respectively, Wilcoxon test $P<0.001$); and (c) the width of V_4 in *G. omarorum* is longer than in *Gymnotus* sp.: the point at which the waveform crosses a threshold set parallel to the abscissa at 20% of the peak ranged from 0.6 to 0.89 ms for *G. omarorum* and from 0.34 to 0.56 ms for *Gymnotus* sp. (Wilcoxon test $P<0.001$). These differences cause an increase in the relative power at higher frequencies in *Gymnotus* sp. (Fig. 1C, light grey power spectrum).

The htEOD in air

In the air gap recordings, current amplitude and voltage amplitude of the directly neurally driven wave components changed in opposite directions according to a decaying linear relationship when different external loads were applied (Fig. 2). The voltages *vs* current plots were referred to as the characteristic function of the source (Fig. 2). The parameters of these functions allowed us to estimate the EMFs as the ordinate intersections and the internal resistances as the slopes (Cox and Coates, 1938; Bell et al., 1976; Caputi et al., 1989).

We did not find any significant differences in the EMF between the two taxa [V_1: 31±5 mV and 26±6 mV; V_2: 175±35 mV and 176±44 mV; V_3: 2.78±0.43 V and 2.63±0.33 V; mean and standard deviation for *G. omarorum* (N=18) and *Gymnotus* sp. (N=15), respectively, Mann–Whitney U-test $P>0.99$ in all cases].

Internal resistance decreases with total length due to a scaling effect. Length-normalised resistance, expressed in resistivity units, was calculated as the product of the internal resistance times the total fish length [for fundamentals, see Caputi and Budelli (Caputi and Budelli, 1995)]. These internal resistance indexes were similar in both species (1289±649 kΩ cm for *G. omarorum*, N=18, and 1349±547 kΩ cm for *Gymnotus* sp., N=15; Mann–Whitney U-test, P=0.47).

In *Gymnotus* sp. (14 out of 15 specimens), V_4 (voltage) *vs* I_4 (current) plots were well fitted by a straight line (Fig. 3A, in all specimens $R^2>0.99$; N always >170). Interestingly, the internal resistance calculated for V_4 was always smaller than the internal resistance calculated for V_3 in the same fish (Wilcoxon test, $P<0.01$, N=14, note the difference in slope compared with V_3, Fig. 3A). Linearity observed was maintained when the same specimens were recorded again after five months of captivity in the lab (N=2). The

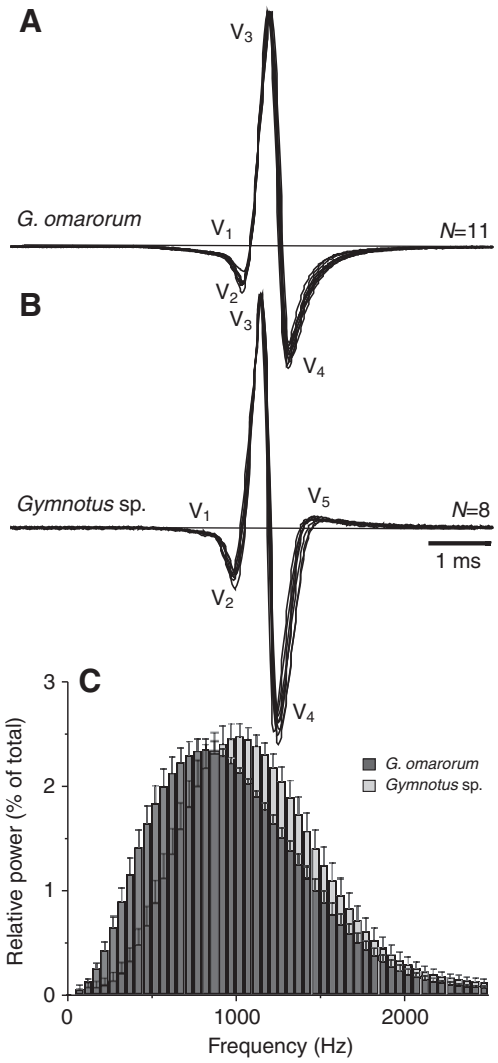

Fig. 1. Head to tail electric organ discharge (EOD) recorded in water. The typical EOD of *Gymnotus omarorum* (A) and *Gymnotus* sp. (B) are compared as recorded by a pair of electrodes placed on the longitudinal axis of the fish at about 1 fish length from the head and the tail, respectively. Note the sharpness of the late negative component (V_4) in *Gymnotus* sp. and the lack of V_5 in *G. omarorum*. (C) The superimposed spectra show a shift to a high frequency range in *Gymnotus* sp.

V_5 (voltage) *vs* I_5 (current) plot showed always non-linear concave relationship resembling a parabola (Fig. 3A).

In *G. omarorum* V_4 (voltage) *vs* I_4 (current) plots showed in most cases a non-linear relationship. The slope of the characteristic function became less steep with the increase of load resistance and in some cases became flat or even inverted for very large resistances (Fig. 3B). In such cases the characteristic function resembled a parabola with a maximum.

Consistently, with these differences, the ratio between V_4 and V_3 (in both species) and between V_5 and V_3 (in *Gymnotus* sp.) always decreased as a function of the external load. The range of this ratio and the slope of the function were different for both species (Fig. 3C). This indicates that external load was an important factor for determining waveform, shape and amplitude of V_4 in *G. omarorum* and also had some influence on V_4 and V_5 in *Gymnotus* sp. This non-linearity exhibited by V_4 in *G. omarorum* and the presence of

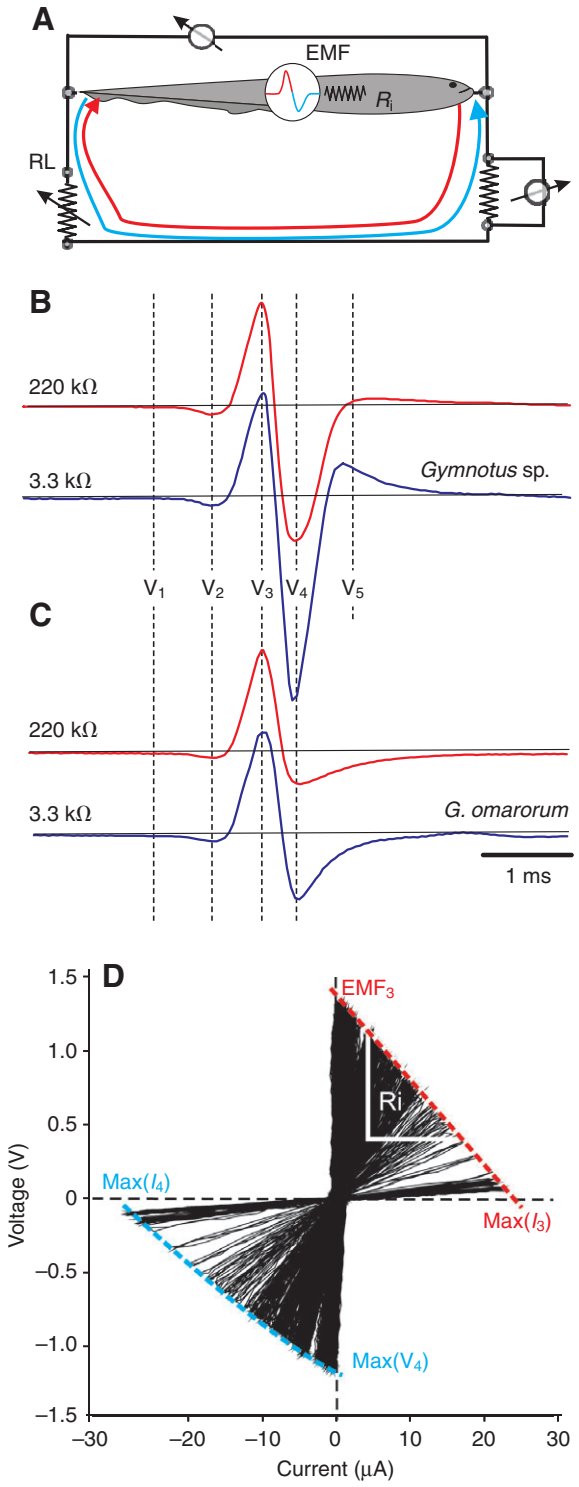

Fig. 2. Head to tail electric organ discharge (htEOD) recorded in air. (A) Equivalent circuit of the fish body as an electric source when a resistive load is applied. Typical htEOD waveforms (normalised to the peak) of *Gymnotus* sp. (B) and *Gymnotus omarorum* (C) are compared as recorded by a pair of electrodes placed on the jaw and the tip of the tail while the fish is maintained in air. The traces in red show the waveforms when the load resistor between the recording electrodes was 220 kΩ. The traces in blue show the waveforms when the load resistor between the recording electrodes was 3.3 kΩ. Note the similarity between the three earlier components V_1, V_2, V_3 and the differences in V_4 and V_5. (D) The plot shows superimposed traces obtained using different values of R1. The point of interception of the ordinate with the straight line passing along the points corresponding to the pick voltages and peak currents (broken red line) is the electromotive force (EMF_3) of the equivalent source at the peak of V_3. The absolute value of the slope of such line corresponds to the internal resistance (R_i) of the equivalent source at the peak of V_3. Because of the non-linear behaviour of V_4 (broken blue line) and V_5, this method only allowed us to estimate these parameters for V_3.

V_5, which is also non-linear, in *Gymnotus* sp. indicate that waveform differences are related to the mechanisms involved in the generation of non-neurally driven components.

Based on earlier studies (Bennett and Grundfest, 1959; Macadar et al., 1989) showing that in *G. carapo* and *G. omarorum* V_4 is generated by the activation of the rostral faces of the electocytes by the action currents generating V_3, we interpreted that the differences between the two studied taxa could be explained by differences in the auto-excitability of the EO and conducted the following experiments to test this hypothesis. First, we showed that V_1, V_2 and V_3 and the EOs were indistinguishable when comparing the two populations under the scope of three different techniques: histological analysis of silver impregnated samples, multiple air gap and multiple air gap under curare. Second, we showed that the amplitude and duration of the late components are functions of the longitudinal currents associated with V_3 (I_3). Whereas in *G. omarorum* the manipulation of I_3 causes a large effect on EMF_4, in *Gymnotus* sp. it causes a very small effect.

The similarities of EOs and the EODs in intact and curarised individuals

Three different techniques allowed us to show similarities between the innervation patterns of EOs and the early components (V_1 to V_3) of the EOD waveform: (a) histological analysis of silver impregnated tissue samples revealed that the EOs show similar structures and innervation patterns in both species; (b) multiple air gap recordings show that EMF patterns mainly differ in the amplitude and shape of the late wave components (V_4 and V_5); and (c) curarisation allowed us to show the similarity between both taxa when the remnants of the EOD achieved a stabilised waveform in which V_4 and V_5 were absent (see Materials and methods). Figs 4–6 show only small differences between both taxa in the innervation patterns, the corresponding regional waveforms and their remnants obtained from the same specimen after partial curarisation.

Transverse sections of the abdominal region show that in both species the EO is composed of four tubes (two on each side) located in the abdominal wall. In *G. omarorum* these tubes are composed of cuboidal electrocytes lying on a single surface parallel to the skin. In *Gymnotus* sp. these tubes have a triangular section. They are arranged in such a way that the lateral faces of lateral electrocytes have a topological arrangement in regard to the peritoneum, and the inferior faces of medial electrocytes lie against the skin (schemata Fig. 4A). Lateral electrocytes are doubly (rostral and caudally) innervated whereas the medial ones are innervated only on the caudal face (Fig. 4A–D). This similarity between anatomies is well matched with the similar waveforms of the abdominal EOD: a smooth V_1 to V_3 pattern is present in both intact and curarised animals. This V_1 to V_3 pattern is followed in the intact animals by a small V_4. In curarised animals the EODs are relatively much smaller and less sharp. V_3 is smaller because the synaptic potential, as indicated by V_1, which is smaller due to curare, and the smaller synaptic potentials do not evoke action potentials on the innervated faces reliably. In addition, V_1 is a long-lasting wave and V_3 occurs during the final portion of V_1 (Fig. 4E).

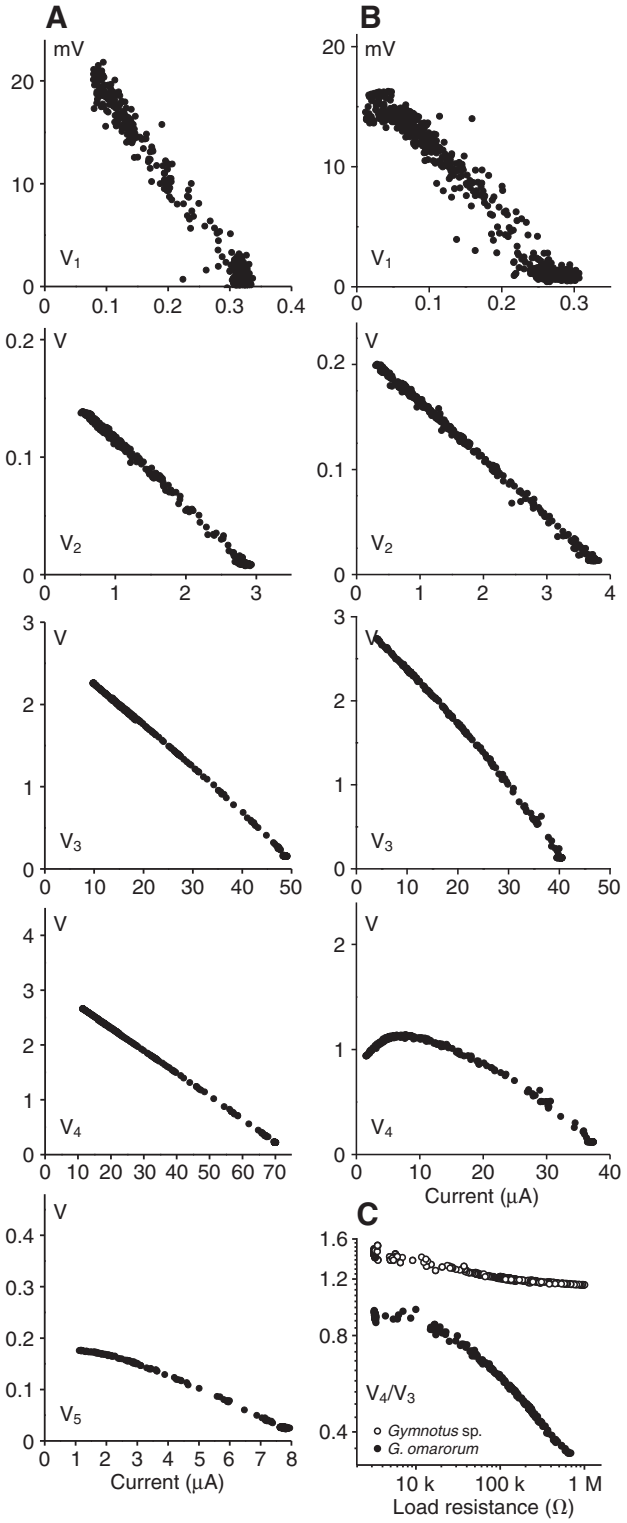

Fig. 3. Characteristic curves. (A) Peak voltage *vs* peak current plot comparing V_1, V_2, V_3, V_4 and V_5 for *Gymnotus* sp. (B) Peak voltage *vs* peak current plot comparing V_1, V_2, V_3 and V_4 for *Gymnotus omarorum*. When the data points were well fitted by a line the ordinate intersection corresponded to the electromotive force (V_1, V_2, V_3 and V_4 in *Gymnotus* sp. and V_1, V_2 and V_3 in *G. omarorum*). Abscissas and ordinates were proportionally adjusted in such a way that equal geometrical slopes mean the same internal resistance in all plots. (C) The ratio V_4/V_3 as a function of the external load in both species (open symbols: *G. omarorum*, closed symbols: *Gymnotus* sp.). Note that load dependence is larger in *G. omarorum*.

In the central region of fish of the two taxa, the EOs are composed of eight tubes (four on each side). They are located on parasagittal planes on either side of the midline. Dorsal electrocytes are larger and extend laterally, partially covering the external face of the electrocyte located below. They are doubly (rostral and caudally) innervated while the others are innervated only caudally (Fig. 5A,B for *G. omarorum* and *Gymnotus* sp.). Consistently with the presence of doubly innervation, a sharp polyphasic complex was generated at this region in both species. However, while V_2 and V_3 were undistinguishable both in intact and curarised animals, the amplitudes of V_4 were always larger in the intact specimens of *Gymnotus* sp. than in *G. omarorum* (Fig. 5C,D). Once again V_2 and V_3 were reduced while V_4 was abolished in *G. omarorum*. In *Gymnotus* sp., a small remnant was observed in one of the experiments. This result may be explained either by the presence of late activated weak synapses on rostral faces of the doubly innervated electrocytes or more likely by a similar mechanism as the second negative peak observed at the abdominal region (because the apparent remnant of V_3 is shorter and smaller than in *G. omarorum*).

In the caudal region of both taxa the EOs are also composed of eight tubes, four on either side of the midline. Electrocyte density increases markedly in the caudal direction and near the tip of the tail they are very densely packed. Electrocytes are caudally innervated (Fig. 6A,B parasagittal sections) and a large posterior electromotor nerve running rostro-caudally is clearly visible (labelled as PEN in Fig. 6B). The regional EOD is consistent with this innervation pattern (Fig. 6C,D). As before, V_3 is reduced and V_4 is abolished with curare. They are preceded by a small biphasic deflection that corresponds to the activity of the posterior electromotor nerve (Trujillo-Cenóz and Echague, 1989; Caputi et al., 1989).

Quantitative analysis of the spatio-temporal pattern in the multiple-air-gap shows similar EOD waveforms in both taxa. The spatio-temporal patterns show that V_1 is generated abdominally, V_2 is generated in the central regions (gaps 2–6), V_3 is generated all along the body and V_4 and V_5 are mainly generated in the caudal two-sevenths of the body (waveforms were normalised to the positive peak in Fig. 7A,B). The regional waveforms (Fig. 7A,B), the absolute amplitudes of each wave component at every portion (Fig. 7C and D), and the ratios V_4/V_3 (Fig. 7E) all show that the main differences between species occur in the indirectly driven components. In central and caudal regions V_4 is larger and briefer in *Gymnotus* sp., consequently the ratios V_4/V_3 are also larger. V_5 is only present in the caudal regions in *Gymnotus* sp. but not in *G. omarorum*. No differences between taxa were found in the relative timings of V_3 along the EO (Fig. 7F).

Differences in EO auto-excitability between species

Both head to tail recordings and the anatomo-functional analysis made in the previous sections suggest that the main differences between the EOD waveforms are caused by differences in auto-excitability. To test this hypothesis we used a differential loading method to quantify the efficacy of longitudinal currents generating V_3 (referred to as I_3) for exciting the rostral faces and thus eliciting V_4 (see Materials and methods). We used the same air gap recording apparatus connected in a different mode to explore the generation of V_4 either when the external load was constant or where we clamped the value of V_3 by using different loads for V_3 and V_4. Diodes split the circuit into two parallel 'one way' paths of opposite direction (Fig. 8A). When the absolute value of the generated voltage was lower than the thresholds of the Germanium diodes (300 mV), current was minimal. When voltage exceeded 300 mV, current was directed to only one of the paths.

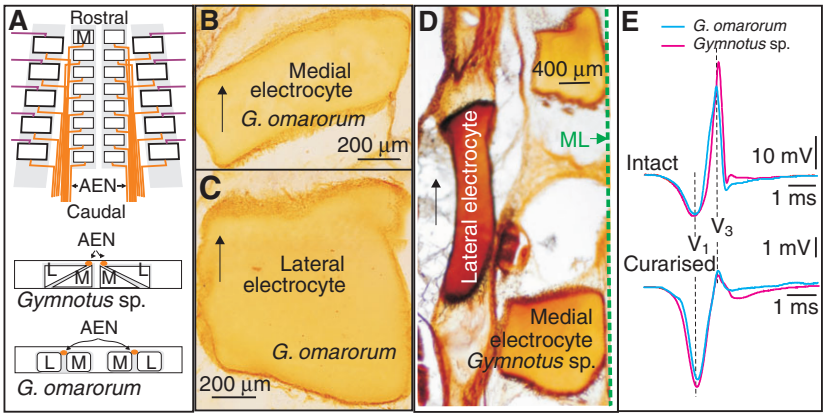

Fig. 4. The abdominal region of the electric organs (EOs) and their electric organ discharges (EODs). (A) Schematics of the innervation pattern of the abdominal portion of the EO. As described by Trujillo-Cenóz and Echague (Trujillo-Cenóz and Echague, 1989), in this region the EO consists of two rows of electrocytes: (i) a lateral row (L) of doubly innervated electrocytes that receive branches of the inter-costal nerves (violet) on the rostral faces and branches of the anterior electromotor nerve (AEN, brown) on the caudal faces, and (ii) a medial row of smaller electrocytes innervated caudally by branches of the AEN. Small differences can be observed in the anatomy: in *Gymnotus* sp. the two tubes on each side are partially stacked in the dorso-ventral direction and the AEN is medial whereas in *Gymnotus omarorum* the two tubes on each side lie side-by-side and the AEN runs between both. (B–D) Microphotographs of silver impregnated parasagittal sections of the EO showing the innervation pattern. Arrows point in the rostral direction. (B) Medial electrocyte in *G. omarorum.* (C) Lateral electrocyte in *G. omarorum.* (D) Medial and lateral electrocytes in *Gymnotus* sp. ML: midline. (E) Regional waveform in the intact fish show that V_1 and V_3 are the principal components. Remnant waveforms after partial curarisation show a different effect on the two components. Blue traces: *G. omarorum*, red traces: *Gymnotus* sp.

When the head to tail drop of voltage was positive the current I_3 flowed through resistor R2 in series with one of the diodes. When the head to tail drop of voltage was negative the current I_4 flowed through resistor R1 in series with the other diode. This network allowed us to clamp the peak of I_3 at a chosen value by setting the value of resistor R2. We set the value of R2 (and consequently clamped the peak current of I_3, max I_3, Fig. 8B) at several values in each of the studied fish (typically from 6 in the field to 11 in the lab). With I_3 clamped, we then constructed a plot of V_4 *vs* I_4 (referred to as the characteristic function plot) by gradually varying the value of the load rheostat R1. As shown in Fig. 8B, the current–voltage plots were superimposed following a slope equal to R2 in the positive–positive quadrant. For negative values of the two variables, the traces followed different slopes as R1 was changed. For each one of the chosen R2 values we constructed a plot of the peak values of V_4 *vs* the peak values of I_4. These plots correspond to the envelopes of the brown and violet graphs of Fig. 8B. We found for all R2 values that this envelope was a line of equal slope but which

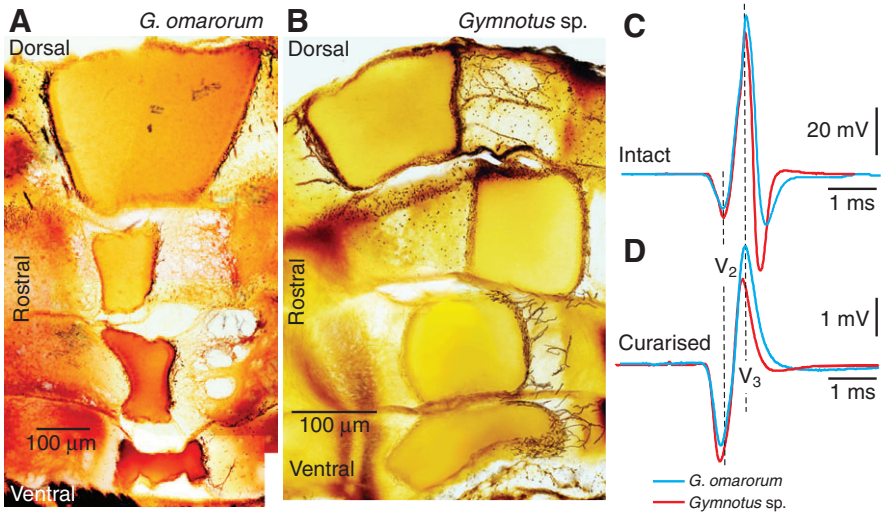

Fig. 5. The central region of the electric organs (EOs) and their electric organ discharges (EODs). (A) Microphotograph of a silver impregnated parasagittal section of the EO showing the innervation pattern of the central portion in *Gymnotus omarorum.* As described by Trujillo-Cenóz and Echague (Trujillo-Cenóz and Echague, 1989) the EO consists of four rows of electrocytes on each side: a dorso-lateral row of doubly innervated electrocytes that receive terminals on their rostral faces and caudal faces and three rows of singly caudally innervated electrocytes. (B) Microphotograph of a silver impregnated parasagittal section of the EO showing the innervation pattern of the central portion in *Gymnotus* sp. Note that the differences in relative size of the dorso-lateral electrocytes are due only to the different orientation and distance from the midline of the sectioning plane. (C) Regional waveform in the intact fish show a three phasic pattern (V_2, V_3, V_4) in both taxa and a large difference in V_4. (D) Remnant waveforms after partial curarisation show the similarity of the EOD remnants. Blue traces: *G. omarorum*; red traces: *Gymnotus* sp.

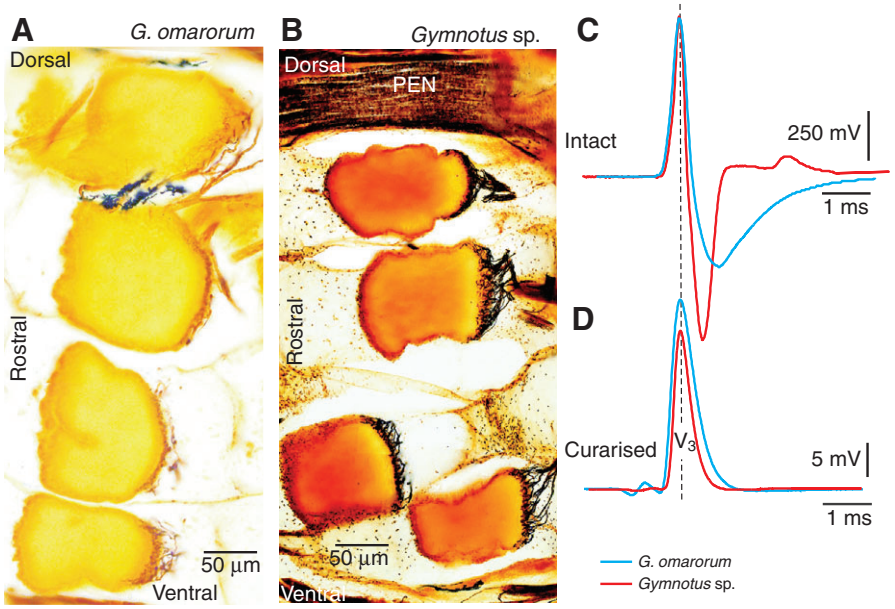

Fig. 6. The tail region of the electric organs (EOs) and their electric organ discharges (EODs). (A) Microphotograph of a silver impregnated parasagittal section of the EO showing the innervation pattern of the tail portion in *G. omarorum*. As described by Trujillo-Cenóz and Echague, in this region the EO consists of four rows of caudally innervated electrocytes on each side (Trujillo-Cenóz and Echagüe, 1989). (B) Microphotograph of a silver impregnated parasagittal section of the EO showing the innervation pattern of the tail portion of the EO in *Gymnotus* sp. (C) Regional waveform in the intact fish shows a biphasic pattern (V_3 and V_4) in both taxa and a large difference in V_4. (D) Remnant waveforms after partial curarisation show the similarity of the EOD remnants after the abolition of V_4. Blue traces: *G. omarorum*; red traces: *Gymnotus* sp.

intersected the ordinate at different values (Fig. 8B and Fig. 9A,B). Thus, non-linearity observed in the simple air gap was a consequence of an increase in EMF_4 due to the increase in the stimulus intensity (I_3). In *G. omarorum* the ordinate intersection (i.e. the equivalent EMF, EMF_4) increased as a function of the amplitude of I_3 (Fig. 9A,C). This was also true for *Gymnotus* sp. although the change in electromotive was much smaller and sometimes null (Fig. 9B,C).

EMF_4 data normalised to their maxima were plotted *vs* normalised I_3. We compared the relationship exhibited by *Gymnotus* sp. (Fig. 10A) with the relationships exhibited by *G. omarorum* gathered at three different seasons (autumn, early spring and late spring, Fig. 10B–D). The auto-excitability may be measured in these plots as the ratio between the minimal EMF measured in open circuit and maximal EMF measured at closed circuit. This auto-excitability index is equivalent to the (I_3=0, R2→∞). The histograms of the auto-excitability indexes show very different shapes: it is unimodal and exhibits small dispersion in *Gymnotus* sp. and is bimodal and exhibits large dispersion in *G. omarorum* (Fig. 10E). We found a large difference between medians and dispersion of auto-excitability index between the two taxa (Wilcoxon test, P<0.001; auto-excitability index range: 0.8–1 for *Gymnotus* sp. and 0.3–0.85 for *G. omarorum*).

Cumulative frequency plots also show these differences between the two taxa and the similarity between the populations of *G. omarorum* gathered and studied at different seasons just after capture or in captivity. Two comparisons were performed: (a) fish studied 24–48 h after capture (black symbols, Fig. 10F) with fish under captivity for more than three months (grey symbols, Fig. 10F, Wilcoxon test, P>0.95); and (b) the freshly gathered fish population according to the season of gathering (autumn=circles, spring=squares and late spring=triangles, Fig. 10F, Kruskal–Wallis test P>0.95). Two specimens of *Gymnotus* sp. were studied twice, immediately after being bought from local dealers in Argentina and after five months in captivity at the lab. Results of both measurements were very similar.

DISCUSSION

The present study compares two taxonomic units, which may be confused at first sight as members of the same taxon. Indeed, the local names for these fish are ‘morena’ in both Argentine Mesopotamia and Uruguay. However, we found that the electric field and the generation mechanisms of the EOD of animals bought in La Paz, Argentina, have phenotypic traits that make it possible to differentiate them from animals captured in Laguna del Cisne, Uruguay. In addition, parallel research (W. G. R. Crampton and J. S. Albert, personal communication) indicates that these populations may represent different taxa. The population found in Uruguay, previously identified as *G. carapo*, is the best studied species of *Gymnotus* and may correspond to a new species, referred to as ‘omari’ as a tribute to Omar Macadar and Omar Trujillo-Cenóz who pioneered research on these fish in Uruguay during the 1980s (Richer de Forges et al., 2009) [for reviews on electromotor and electrosensory systems of this taxon, see Caputi (Caputi, 1999) and Caputi et al. (Caputi et al., 2008)]. The population found in Argentina (and also reported in the south of Brazil and Paraguay) may also correspond to a new species, *Gymnotus* sp.

The main difference between EOD waveforms recorded head to tail in water appears in the late components (V_4 in *G. omarorum* and V_4 and V_5 in *Gymnotus* sp.). These differences determine the shift of the power spectrum to a higher frequency range. Previous evidence indicates that V_4 in *G. omarorum* is generated by the indirect activation of the membranes of the rostral faces of the electrocytes. Intracellular recordings obtained from *in vitro* preparations of the EO show that action currents generated by the activation of caudal faces triggered the generation of action potentials on the rostral faces (Bennett, 1971; Macadar et al., 1989; Lorenzo et al., 1988; Sierra, 2007) but not on the lateral faces (Sierra, 2007; Markham and Stoddard, 2005). Net action currents generated by the delayed activation of the rostral faces flow from caudal to rostral through the muscle and other non-excitable tissues of the fish, as well as through the surrounding water, and contribute to V_4.

The following evidence indicates that the differences in EOD waveform reported here result from differences in the EO auto-excitability in the two taxa.

Firstly, we did not found major differences in the early components of the EOD waveforms of *G. omarorum* and *Gymnotus* sp. either in the intact or curarised specimens. Moreover, curarisation experiments showed that V_4 and V_5 in *Gymnotus* sp. and V_4 in *G.*

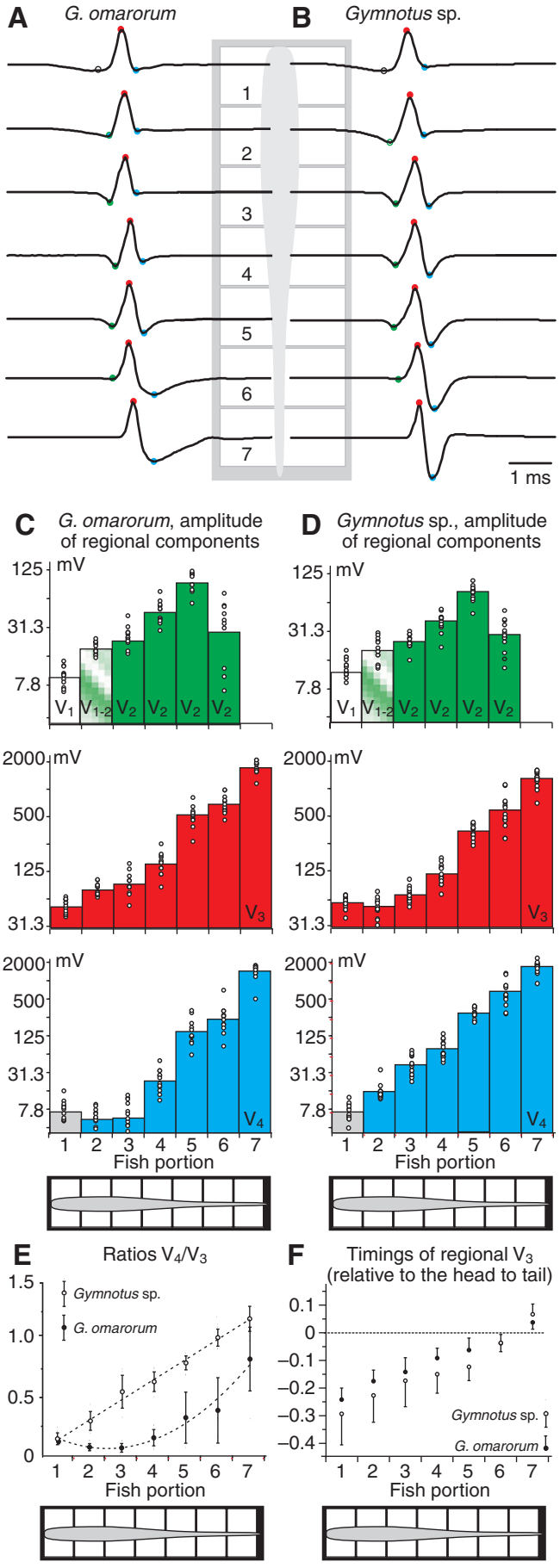

Fig. 7. Spatio-temporal pattern of the electric organ discharge (EOD). (A) *Gymnotus omarorum* and (B) *Gymnotus* sp.: regional EOD normalised waveforms were obtained from seven contiguous portions of the body using the air gap system. Both taxa show a similar smooth V_1 (white) in portion 1 and 2, a sharp negative V_2 (green) in portions 2–6 and a positive V_3 (red) all along the fish. Note that in *G. omarorum,* V_4 (blue) is relatively smaller and has a longer duration in gaps 6 and 7. Colour dots in A and B indicate site of peak measurement (same colour code as in C and D). (C) *G. omarorum* and (D) *Gymnotus* sp.*:* amplitude of regional components. Data from eight fish of each taxon studied in the autumn. Note that in *G. omarorum,* V_4 is smaller in absolute terms in all portions, particularly in the rostral ones. Same colour code as in A and B. The top plots combine data from V_1 (white column) and V_2 (green columns). Combined grey white columns correspond to a body portion that generates both V_1 and V_2; E) Comparison between ratios V_4/V_3 for all the gaps (same eight fish of each taxon). (F) Timings of the regional V_3 as a function of the portion of origin. Note the similar rostro-caudal progression of the activation volley.

omarorum (Caputi et al., 1989) were abolished at the tail region. This result has been observed in other gymnotids such as *B. pinnicaudatus* (Caputi et al., 1998), and *Rhamphychthys rostratus* (Caputi et al., 1994) at the tail region where only caudally innervated electrocytes occur. Curare diminishes the synaptic potentials and thus the likelihood and synchronism of action potentials on the innervated face. This causes a smooth reduction of the V_1, a wave component generated at synaptic potentials, but disorganisation of the sharp complex including V_2, V_3, V_4 and V_5 generated by action currents. When curarisation reaches the stabilised stage the amplitude decays gradually without changes in waveform because the EOD remnant corresponds to sub-threshold synaptic potentials. Thus, the similarity of profiles at this stabilised stage of partial curarisation suggests that the neural activation volleys are similar in both species.

A second indication that the differences in EOD waveform result from differences in auto-excitability comes from the sensitivity of late wave components to load. In the case of the directly neurally driven components (V_2 and V_3), modelling based on linear sources accurately represents the data obtained in the simple air gap experiments. However, in the case of indirectly neurally driven components (V_4 and V_5) EMFs were load dependent. The auto-excitability hypothesis also predicts the increase in duration and the relative amplitude decrease of V_4 and V_5 observed in the recordings in air. Because the relative changes in peak amplitude are larger than changes in the overall area of the EOD waveform, this suggests that the main difference between the two taxonomic units is a different degree of synchrony in the activation of the rostral faces. These findings indicate that the EMF_4 depends on the current associated with V_3. This dependence is more marked in *G. omarorum* and does not vary with either seasonal conditions or time in captivity.

The third and strongest evidence that the differences in EOD waveform results from differences in auto-excitability was obtained by using the technique of differential loading. We showed that when the current associated with V_3 was clamped at a given value (I_3), the data points of the characteristic plot for V_4 were well fitted by a line whose ordinate (or electromotive force, EMF4) depended on the clamped value of I_3. This procedure demonstrates a cause–effect relationship between the process generating V_3 and the process generating V_4 and confirms the hypothesis of a generation mechanism based on the auto-excitability of the EO. Due to the smaller value of V_5 and the threshold of 0.3 mV characteristic of Germanium diodes, we were unable to make the same analysis in the case of V_5. Nevertheless, its similar behaviour in the simple air

gap suggests that this component is also generated by an auto-excitation mechanism.

The differential loading technique also allowed us to quantify the auto-excitability of the EO using an index that is easy to obtain in the intact fish and therefore a powerful tool for comparing auto-excitability within and between fish populations. Index comparison clearly showed that the differences in waveforms between *Gymnotus* sp. and *G. omarorum* reflect the differences in the auto-excitability

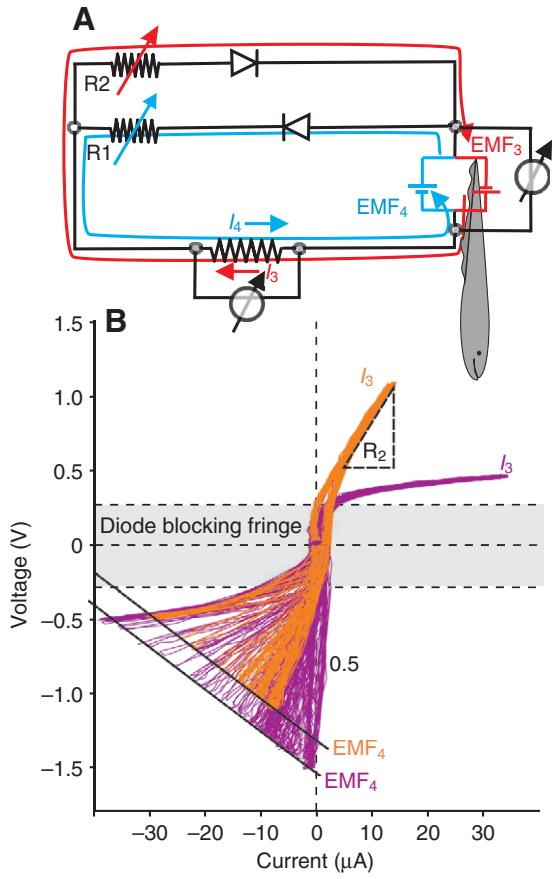

Fig. 8. Estimation of the electromotive force (EMF) driving V_4 with the differential load method. (A) Diagram of the recording circuit. The limits of the explored body portion were connected to a recording network consisting of two parallel 'one way' resistive branches. The direction of the current flow (red I_3, blue I_4) at each branch was defined by the orientation of a diode connected in series with the load resistors (R1 and R2). The sum of currents flowing through the two branches was evaluated as the drop of voltage across a resistor connected in series divided its value (3.3 kΩ). The voltage was measured between the two electrodes contacting the explored body portion. (B) Plots of the voltage *vs* current. Loops of different shape are generated at different values of R1 (each loop corresponds to a single EOD) and R2. In the present study we show more than 100 loops corresponding to different positions of the rheostat on each run. Brown and violet traces were obtained for different values of R2. The grey band indicates the diode blocking fringe (±0.3 V) where current flowing through the circuit is minimal. Above, the fringe loops follow a linear trajectory whose slope represents the value of R2. This value sets the maximum value of I_3 (in the example the brown line corresponds to a larger R2). Below the fringe loops follow a linear trajectory in which the slope represents the value of R1. Changes in R1 allowed us to construct the characteristic curve of V_4 for each of the selected values of R2. Note that when R2 is larger (brown lines), I_3 and the ordinate intersection are smaller than when R2 is smaller (violet traces). The slopes of the brown and violet envelopes are the same indicating that internal resistance of the fish body is the same.

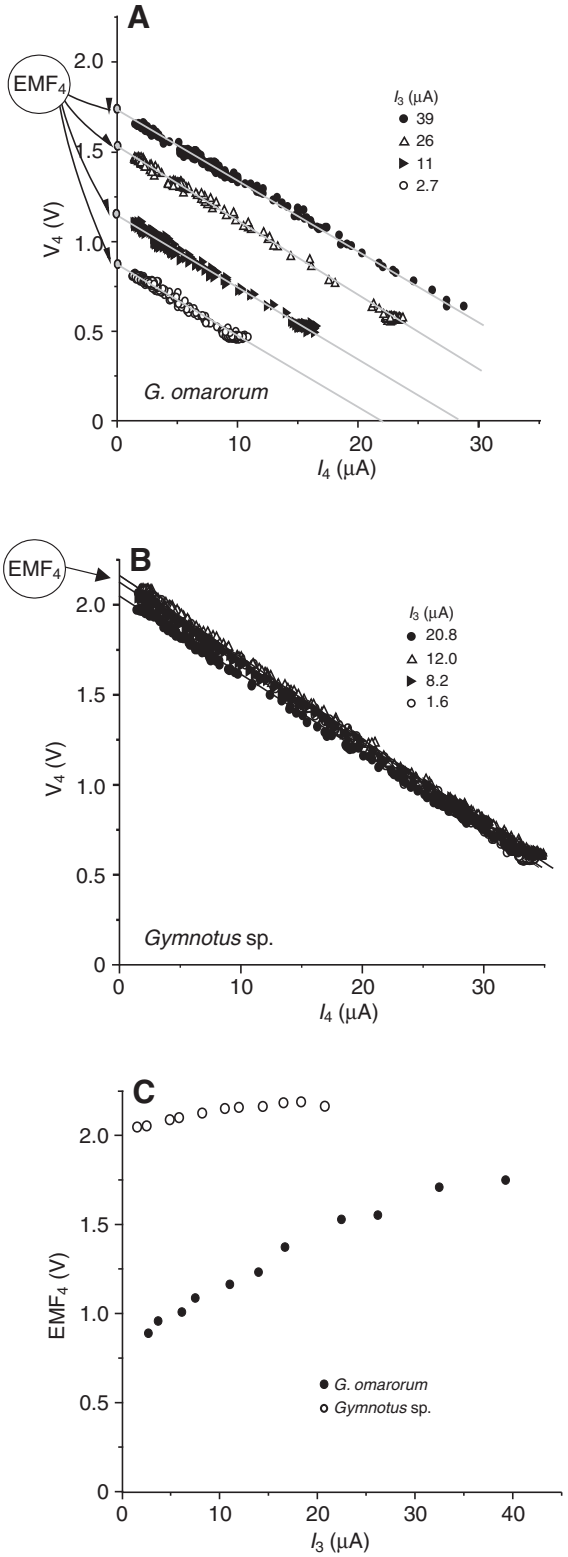

Fig. 9. The electromotive force (EMF) of the V_4 equivalent source depends on the intensity (I_3) of external current flowing during V_3. (A) V_4 peak voltage *vs* peak current (I_4) plots evaluated for four values of I_3 in *Gymnotus omarorum*. Note the similarity in slope and the difference in ordinate intercept (electromotive force, EMF). (B) V_4 *vs* I_4 plots evaluated for four values of I_3 in *Gymnotus* sp. Note the similarity in slope and also in EMF. (C) EMF_4 as a function of I_3 (closed symbols *G. omarorum*; open symbols *Gymnotus* sp.). Note that the relative increase in EMF4 in *G. omarorum* is larger than in *Gymnotus* sp.

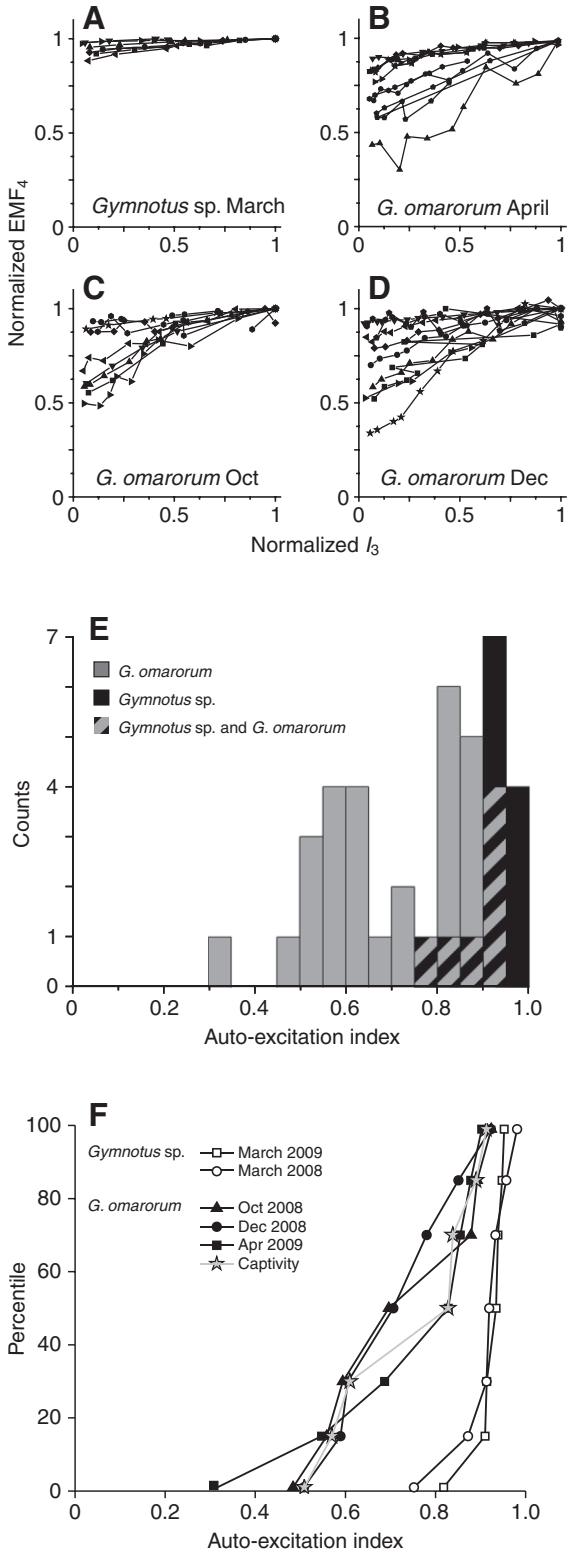

Fig. 10. Differences in auto-excitability. (A–D) Normalised EMF_4 as a function of normalised I_3 (*Gymnotus* sp.*:* A; *Gymnotus omarorum* studied just after gathering at three different seasons: B–D). (E) Comparison between the histograms of the auto-excitability indexes (grey, *G. omarorum*; black, *Gymnotus* sp.; the cross-hatched shading indicates the superposition of the two histograms). (F) Cumulative distributions of the auto-excitability indexes of four populations of *G. omarorum* (freshly caught: black; after several months in captivity: grey) and two populations of *Gymnotus* sp. (open symbols).

of their EO. Interestingly, *G. omarorum* has a wide range of auto-excitability that marginally overlaps with that of *Gymnotus* sp., showing either a genetic heterogeneity or a local environmental factor affecting genotypic expression. Moreover, the similar distribution of auto-excitability indexes of *G. omarorum* when comparing fish in captivity *vs* freshly caught fish or fish gathered in different seasons indicate that wide dispersion is a characteristic of the taxon.

Although this study was not designed to discriminate the contributions of the different factors involved in auto-excitability, our data suggest that the ion channel repertoire, either in the electrocyte membrane or in the connective tissue tubes that encase them, may be the most important element in the taxonomic units that are compared.

We conclude that the differences in the EOD phenotype of the two studied taxa are due to the different expression of a genetic repertoire of voltage-dependent conductances in the rostal electrocyte membranes and/or leakage conductances in the connective sheath encasing the electrocytes. Regardless the possibility of a parapatric speciation process, the observed EOD waveform diversity may be useful for avoiding hybridisation along the borders of neighbouring geographic ranges and for reinforcing pre-existing differences.

This work was funded in part by grant DEB 0614334 from the national Science Foundation (USA); a grant from the European Commission ICT-FET proactive initiative 'embodied intelligence' (Project acronym: ANGELS, Grant No. 231845) and PEDECIBA (Uruguay). The authors wish to thank Daniela Hadasch and Mirjam Holbach for their help in the development of the differential load technique, Lic. Alejandra Pastorino for technical assistance with histological procedures, and Dr Kirsty Grant for help with the English and useful comments. Authorship: Experiments: A.R.-C. and A.A.C.; study design and manuscript writing: A.A.C. The results presented in this article form a substantial part of the MSc Thesis of A.R.-C.

REFERENCES

Albe-Fessard, D. and Buser, P. (1950). Étude de l'interaction par champú électrique entre deux fragments d'organe de torpille (*Torpedo marmorata). J. Physiol.* (*Paris*) **42**, 528-529.

Albert, J. S. and Crampton, W. (2005). Diversity and phylogeny of neotropical electric fishes (Gymnotiformes). In *Electroreception* (ed. T. H. Bullock, C. D. Hopkins, A. N. Popper and R. R. Fay), pp. 360-409. New York: Springer.

Bass, A. H. (1986). Electric organs revisited: evolution of a vertebrate communication and orientation organ. In *Electroreception* (ed. T. H. Bullock and W. Heiligenberg), pp. 13-70. New York: Wiley.

Bass, A. H. and Hopkins, C. D. (1983). Hormonal control of sexual differentiation: changes in electric organ discharge waveform. *Science* **220**, 971-974.

Bell, C. C., Bradbury, J. and Russell, C. J. (1976). The electric organ of a mormyrid as a current and voltage source. *J. Comp. Physiol.* **110A**, 65-88.

Bennett, M. V. L. (1971). Electric organs. In *Fish Physiology*, vol. V (ed. W. S. Hoar and D. J. Randall), pp. 347-491. London: Academic Press.

Bennett, M. V. L. and Grundfest, H. (1959). Electrophysiology of electric organ in *Gymnotus carapo. J. Gen. Physiol.* **42**, 1067-1104.

Bullock, T. H., Hagiwara, S., Kusano, K. and Negishi, K. (1961). Evidence for a category of electroreceptors in the lateral line of gymnotid fishes. *Science* **134**, 1426-1427.

Caputi, A. A. (1999). The EOD of pulse gymnotiforms, from a single impulse to a complex electromotor pattern. *J. Exp. Biol.* **202**, 1229-1241.

Caputi, A. and Aguilera, P. (1996). A field potential analysis of the electromotor system in *Gymnotus carapo. J. Comp. Physiol.* **179A**, 827-835.

Caputi, A. and Budelli, R. (1995). The electric image in weakly electric fish. I. A data-based model of waveform generation in *Gymnotus carapo. J. Comput. Neurosci.* **2**, 131-147.

Caputi, A., Macadar, O. and Trujillo-Cenóz, O. (1989). Waveform generation in *Gymnotus carapo*. III. Analysis of the fish body as an electric source. *J. Comp. Physiol.* **165A**, 361-370.

Caputi, A., Silva, A. and Macadar, O. (1993). Electric organ activation in *Gymnotus carapo*: spinal and peripheral mechanisms. *J. Comp. Physiol.* **173A**, 227-232.

Caputi, A., Macadar, O. and Trujillo-Cenóz, O. (1994). Waveform generation in *Rhamphichtys rostratus* (L.) (Teleostei, Gymnotiformes). The electric organ and its spatiotemporal activation pattern. *J. Comp. Physiol.* **174A**, 633-642.

Caputi, A., Silva, A. and Macadar, O. (1998). The effect of environmental variables on waveform generation in *Brachyhypopomus pinnicaudatus. Brain Behav. Evol.* **52**, 148-158.

Caputi, A. A., Carlson, B. A. and Macadar, O. (2005). The electric organs and their control. In *Electroreception* (ed. T. H. Bullock, C. D. Hopkins, A. N. Popper and R. R. Fay), pp. 410-452. New York: Springer.

Caputi, Á. A., Castelló, M. E., Aguilera, P. A., Pereira, A. C., Nogueira, J., Rodríguez-Cattaneo, A. and Lezcano, C. (2008). Active electroreception in

Gymnotus omari: Imaging, object discrimination, and early processing of actively generated signals. *J. Physiol. (Paris)* **102**, 256-271.
Coates, C. W., Cox, R. T. and Granath, L. P. (1937). The electric discharge of the electric eel, *Electrophorus electricus* (Linnaeus). *Zoologica* **22**, 1-34.
Coates, C. W., Altamirano, M. and Grundfest, H. (1954). Activity in electrogenic organs of knifefishes. *Science* **120**, 845-846.
Couceiro, A. and De Almeida, D. F. (1961). The electrogenic tissue of some gymnotidae. In *Bioelectrogenesis* (ed. C. Chagas and A. Paes de Carvalho), pp. 3-13. Amsterdam: Elsevier.
Cox, R. T. and Coates, C. W. (1938). Electrical characteristics of the electric tissue of the electric eel *Electrophorus electricus* (Linnaeus). *Zoologica* **23**, 203-212.
Crampton, W. G. R. and Albert, J. S. (2005). Evolution of electric signal diversity in the gymnotiform fishes. In *Fish Communication* (ed. S. P. Collin, B. G. Kapoor, F. Ladich and P. Moller), pp. 360-403. New York: Science Publishers.
Crampton, W. G. R., Davis, J. K., Lovejoy, N. R. and Pensky, M. (2008). Multivariate classification of animal communication signals. A simulation based comparison of alternative of signal process procedures using electric fishes. *J. Physiol.* (*Paris*) **102**, 304-321.
Darwin, C. R. (1866). On the origin of species by means of natural selection, or the preservation of favoured races in the struggle for life (2nd edition). In *The Complete Work of Charles Darwin.* London: John Murray. Online http://Darwinonline.org.uk.
Hopkins, C. D. (1999). Design features for electric communication. *J. Exp. Biol.* **202**, 1217-1228.
Hopkins, C. D., Comfort, N. C., Bastian, J. and Bass, A. H. (1990). Functional analysis of sexual dimorphism in an electric fish, *Hypopomus pinnicaudatus*, order Gymnotiformes. *Brain Behav. Evol.* **35**, 350-367.
Lissmann, H. W. (1951). Continuous electrical signals from the tail of a fish, *Gymnarchus niloticus* Cuv. *Nature* **167**, 201-202.
Lissmann, H. W. (1958). On the function and evolution of electric organs in fish. *J. Exp. Biol.* **35**, 156-191.
Lissmann, H. W. and Machin, K. E. (1958). The mechanism of object location in *Gymnarchus Niloticus* and similar fish. *J. Exp. Biol.* **35**, 451-486.
Lorenzo, D., Velluti, J. C. and Macadar, O. (1988). Electrophysiological properties of abdominal electrocytes in the weakly electric fish *Gymnotus carapo*. *J. Comp. Physiol.* **162**, 141-144.
Macadar, O., Lorenzo, D. and Velluti, J. C. (1989). Waveform generation of the electric organ discharge in *Gymnotus carapo.* II. Electrophysiological properties of single electrocytes. *J. Comp. Physiol.* **165A**, 353-360.
Machin, K. E. and Lissmann, H. W. (1960). The mode of operation of the electric receptors in *Gymnarchus niloticus*. *J. Exp. Biol.* **37**, 801-811.
Markham, M. R. and Stoddard, P. K. (2005). Adrenocorticotropic hormone enhances the masculinity of an electric communication signal by modulating the waveform and timing of action potentials within individual cells. *J. Neurosci.* **25**, 8746-8754.
Mohres, F. P. (1957). Elektrische Entladungen im Dienste der Revierabgrenzung bel Fischen. *Naturwissenschaften* **44**, 431-432.
Ramón y Cajal, S. and De Castro, F. (1933). Elementos de técnica micrográfica del sistema nervioso. Barcelona, Madrid, Buenos Aires: Salvat Editores.
Richer de Forges, M., Crampton, W. G. R. and Albert, J. S. (2009). A new species of *Gymnotus* (Gymnotiformes, Gymnotidae) from Uruguay: description of a model species in neurophysiological research. *Copeia* **2009**, 538-544.
Rodríguez-Cattáneo, A., Pereira, A. C., Aguilera, P. A., Crampton, W. G. R. and Caputi, A. A. (2008). Species-specific diversity of a fixed motor pattern: the electric organ discharge of *Gymnotus*. PLoS ONE, **35**, e2038. doi:10.1371/journal.pone.0002038**.**
Sierra, F. (2007). El órgano eléctrico de *Gymnotus*: Mecanismos iónicos responsables de su descarga, Tesis de Doctorado, PEDECIBA - UDELAR. Montevideo, Uruguay.
Sierra, F., Comas, V., Buño, W. and Macadar, O. (2005). Sodium-dependent plateau potentials in electrocytes of the electric fish *Gymnotus carapo*. *J. Comp. Physiol. A-Sensory Neural and Behavioral Physiology* **191**, 1-11.
Sierra, F., Comas, V., Buño, W. and Macadar, O. (2007). Voltage-gated potassium conductances in Gymnotus electrocytes. *Neuroscience* **145**, 453-463.
Silva, A., Quintana, L., Ardanaz, J. L. and Macadar, O. (2002). Environmental and hormonal influences upon EOD waveform in gymnotiform pulse fish. *J. Physiol.* (*Paris*) **96**, 473-484.
Stoddard, P. K. (1999). Predation enhances complexity in the evolution of electric fish signals. *Nature* **400**, 254-256.
Stoddard, P. K. (2002). The evolutionary origins of electric signal complexity. *J. Physiol.* (*Paris*) **96**, 485-491.
Trujillo-Cenóz, O. and Echagüe, J. A. (1989). Waveform generation of the electric organ discharge in *Gymnotus carapo.* I. Morphology and innervation of the electric organ. *J. Comp. Physiol.* **165**A, 343-351.
Trujillo-Cenóz, O., Echagüe, J. A. and Macadar, O. (1984). Innervation pattern and electric organ discharge waveform in *Gymnotus carapo*. *J. Neurobiol.* **15**, 273-281.
Zakon, H. H., Zwickl, D. J., Lu, Y. and Hillis, D. M. (2008). Molecular evolution of communication signals in electric fish *J. Exp. Biol.* **211**, 1814-1818.